nature immunology

RNA-mediated interference and reverse transcription control the persistence of RNA viruses in the insect model *Drosophila*

Bertsy Goic[1], Nicolas Vodovar[1,3], Juan A Mondotte[1], Clément Monot[2], Lionel Frangeul[1], Hervé Blanc[1], Valérie Gausson[1], Jorge Vera-Otarola[2], Gael Cristofari[2] & Maria-Carla Saleh[1]

How persistent viral infections are established and maintained is widely debated and remains poorly understood. We found here that the persistence of RNA viruses in *Drosophila melanogaster* was achieved through the combined action of cellular reverse-transcriptase activity and the RNA-mediated interference (RNAi) pathway. Fragments of diverse RNA viruses were reverse-transcribed early during infection, which resulted in DNA forms embedded in retrotransposon sequences. Those virus-retrotransposon DNA chimeras produced transcripts processed by the RNAi machinery, which in turn inhibited viral replication. Conversely, inhibition of reverse transcription hindered the appearance of chimeric DNA and prevented persistence. Our results identify a cooperative function for retrotransposons and antiviral RNAi in the control of lethal acute infection for the establishment of viral persistence.

The most well-characterized viral infections are those with human or economic effects. However, regardless of the organism under consideration, there are viruses able to infect that organism. Viral fossil registers highlight the long coevolutionary history between virus and host[1,2]. The outcome of such host-pathogen interactions is highly variable and ranges from deleterious infections with lethal or permanent damage to completely innocuous infections[3]. For example, acute viral infections are characterized by a high rate of viral replication and the production of a large number of progeny. Replication is transient and is limited either by death of the infected cells or by clearance of the virus by the host immune response. In contrast, persistent infections may be the result of an acute primary infection that is not cleared. In this case, the ability of the virus to be transmitted to other organisms or to the offspring of the host is maintained. Persistent infections are at the boundary that separates deleterious infections from innocuous infections. In this unique circumstance, the virus and host use attack and counterattack machinery to reach an equilibrium at which viral infection is controlled but not eliminated. Insect-virus interactions are useful models with which to delineate persistent infections, because many viruses that infect insects develop a persistent infection without obvious fitness costs to the host[4,5]. Furthermore, many persistently infected arthropods, and insects in particular, can act as vectors for emerging viral infectious diseases with considerable medical and economic effects, such as West Nile Virus or Dengue virus[6].

Flock house virus (FHV) belongs to the *Nodaviridae* family and is a nonenveloped virus with a bisegmented genome (RNA1, 3,107 nucleotides; RNA2, 1,400 nucleotides) of positive single-stranded RNA with a 5′ terminal methylated cap and a nonpolyadenylated 3′ end. FHV is a useful viral model because it can produce acute and persistent infections in cell culture as well as in animal models[7,8]. Initial efforts to characterize persistent infections *in vitro* indicated that the FHV genome is unaltered during the establishment of persistence and that mutations of the viral genome begin to accumulate only after multiple passages on persistently infected cells[9]. Of note, mutations accumulate in RNA2, which encodes the coat protein, but not in RNA1, which encodes the viral RNA–dependent RNA polymerase and B2, a strong suppressor of RNA-mediated interference (RNAi)[10]. Those observations suggest that a change in the cellular physiology rather than the virus itself is responsible for establishing the persistent state. However, the molecular and cellular mechanisms underlying this process have remained unresolved. Other studies have associated the appearance of defective interfering particles with persistent infection by FHV[9,11] or other RNA viruses[12–15]. Defective interfering particles are unable to complete a full replication cycle because of genome deletions and consequently need wild-type viruses to replicate their genomes. Such particles can also interfere with the replication of wild-type virus through competition for viral or host factors essential for replication, facilitated by their replicative advantage due

[1]Institut Pasteur, Viruses and RNA Interference, Centre National de la Recherche Scientifique URA3015, Paris, France. [2]Institut National de la Santé et de la Recherche Médicale U1081, Centre National de la Recherche Scientifique Unité Mixte de Recherche 7284, University of Nice–Sophia-Antipolis, Faculty of Medicine, Institute for Research on Cancer and Aging, Nice, Nice, France. [3]Present addresses: Institut National de la Santé et de la Recherche Médicale, Unité Mixte de Recherche en Santé 942, Hôpital Lariboisière, Paris, France; Département de Biologie, Institut de Biologie Génétique et Bioinformatique, Université d'Evry-Val-d'Essonne, Evry, France; Assistance Publique des Hôpitaux de Paris, Hôpital Lariboisière, Service de Biochimie et de Biologie moléculaire, Unité de Biologie Clinique Structurale, Paris, France. Correspondence should be addressed to M.-C.S. (carla.saleh@pasteur.fr).

Received 9 November 2012; accepted 8 January 2013; published online 24 February 2013; doi:10.1038/ni.2542

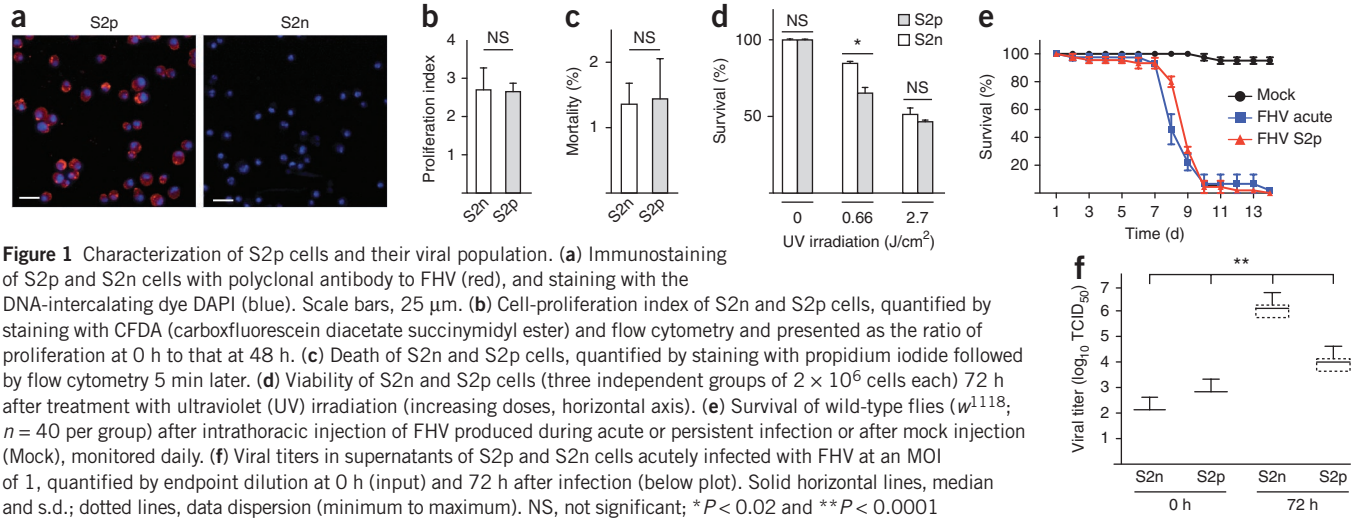

Figure 1 Characterization of S2p cells and their viral population. (**a**) Immunostaining of S2p and S2n cells with polyclonal antibody to FHV (red), and staining with the DNA-intercalating dye DAPI (blue). Scale bars, 25 μm. (**b**) Cell-proliferation index of S2n and S2p cells, quantified by staining with CFDA (carboxfluorescein diacetate succinymidyl ester) and flow cytometry and presented as the ratio of proliferation at 0 h to that at 48 h. (**c**) Death of S2n and S2p cells, quantified by staining with propidium iodide followed by flow cytometry 5 min later. (**d**) Viability of S2n and S2p cells (three independent groups of 2×10^6 cells each) 72 h after treatment with ultraviolet (UV) irradiation (increasing doses, horizontal axis). (**e**) Survival of wild-type flies (w^{1118}; $n = 40$ per group) after intrathoracic injection of FHV produced during acute or persistent infection or after mock injection (Mock), monitored daily. (**f**) Viral titers in supernatants of S2p and S2n cells acutely infected with FHV at an MOI of 1, quantified by endpoint dilution at 0 h (input) and 72 h after infection (below plot). Solid horizontal lines, median and s.d.; dotted lines, data dispersion (minimum to maximum). NS, not significant; $*P < 0.02$ and $**P < 0.0001$ (Student's *t*-test). Data from one experiment representative of four experiments (**a**), three independent experiments (**b**–**d**; mean and s.d.), one experiment representative of three experiments with each condition in triplicate (**e**; error bars, s.d.) or at least eight independent experiments (**f**).

to the smaller size of their genome[16]. It has been suggested that during persistent infection of *Drosophila melanogaster* cells with FHV, the RNA derived from such particles is a chief contributor to the formation of virus-derived small interfering RNA (vsiRNA), because double-stranded RNA (dsRNA) from defective interfering particles could be processed more efficiently by the RNAi machinery than are viral dsRNA replicative intermediates[11,17]. The RNAi machinery is also important in maintaining persistent infections in *Drosophila* cell lines[18]. That study suggests that direct 'dicing' of the viral dsRNA replicative intermediate might be one mechanism that allows control of the viral infection, as the bulk of vsiRNAs are not loaded into the RNA-silencing effector proteins argonaute 1 and argonaute 2 (Ago2). Even if the 'dicing hypothesis' was able to explain how viral replication is controlled during long-lasting infections, it does not explain how the persistent state is established, mainly because that study used cells already persistently infected with FHV.

In this work, we sought to understand how viral persistence is established and maintained in insects. We found that *Drosophila* cells and flies infected with FHV or other positive single-stranded RNA viruses generated DNA of viral origin through endogenous reverse-transcriptase activity. We further demonstrated that those viral DNA forms were transcribed and produced vsiRNAs that 'fed' the RNAi antiviral machinery.

RESULTS

Characterization of persistently infected *Drosophila* S2 cells

To study how viral persistence is established and maintained in insects, we infected naive *Drosophila* S2 cells (S2n cells) by limiting dilution[9,11] with several RNA viruses, including the positive single-stranded RNA viruses FHV and *Drosophila* C virus (DCV), and the dsRNA virus *Drosophila* X virus (DXV; **Supplementary Fig. 1a**). Cells that survived the lytic infection proliferated and remained persistently infected even after 35 passages (**Supplementary Fig. 1b**). We further characterized the S2 cell lines persistently infected with FHV (S2p cells). Immunostaining of S2p cells with antibody to FHV capsid showed that all cells were homogeneously infected by FHV (**Fig. 1a**), which excluded the possibility of the presence of cells refractory to infection. Furthermore, S2p cells did not show a difference in proliferation (**Fig. 1b**) or death (**Fig. 1c**) relative to that of S2n cells, which indicated that persistent infection did not impose any fitness cost on the S2p cell population. To exclude the possibility that the selection of rare initial events contributed to the establishment of persistence independently of the virus, we tested the resistance of S2p cells to apoptosis. Both S2p and S2n cells were similarly sensitive to ultraviolet irradiation (**Fig. 1d**), which indicated that the survival of S2p cells after infection was not due to a defect in apoptosis. We also tested the infectivity of the virus produced by S2p cells. Wild-type (w^{1118}) flies infected with 500 $TCID_{50}$ (half-maximal tissue culture infectious dose) of virus recovered from the supernatants of either S2p cells or acutely infected S2n cells died at a similar rate (**Fig. 1e**), which indicated that persistence was not established from a less-virulent virus population or from a loss of virulence during infection. As neither cell fitness nor FHV virulence was altered in S2p cells, we next hypothesized that the persistence could have resulted from the control of viral replication below a cytopathogenic threshold that would be accompanied by less production of virus in S2p cells[11]. We compared viral titers after acute and persistent infection and observed that viral titers were significantly lower in S2p cells (**Fig. 1f**); accordingly, there was also less accumulation of viral RNA segments during persistent infection (**Supplementary Fig. 1c**). As viral titers varied in S2n cells versus S2p cells, we analyzed differences in the antiviral response. In insects, the main antiviral response acts through the canonical Dicer-2 (endoribonuclease)–Ago2 siRNA pathway[10,19–21]. To assess the antiviral RNAi response in S2p and acutely infected S2n cells, we produced small-RNA libraries and examined the vsiRNA profiles. We found vsiRNAs that mapped all along both FHV genome segments (RNA1 and RNA2; **Supplementary Fig. 1d–g**), which indicated that the RNAi machinery effectively processed the viral dsRNA in both conditions. Together these observations showed that persistently infected cells produced less virus because of control of viral replication by an unknown cellular mechanism.

New cellular synthesis of viral cDNA from viral RNA

RNA from non-retroviral RNA viruses can be reverse-transcribed into cDNA by retrotransposons or endogenous retroviruses[22–30]. The role of non-retroviral DNA forms of RNA viruses remains unresolved, although involvement in immunity has been proposed[25,26]. Hence, we investigated whether RNA viruses generated DNA forms in *Drosophila* cells and whether those DNA forms correlated with the establishment and maintenance of persistent infection. We extracted genomic DNA

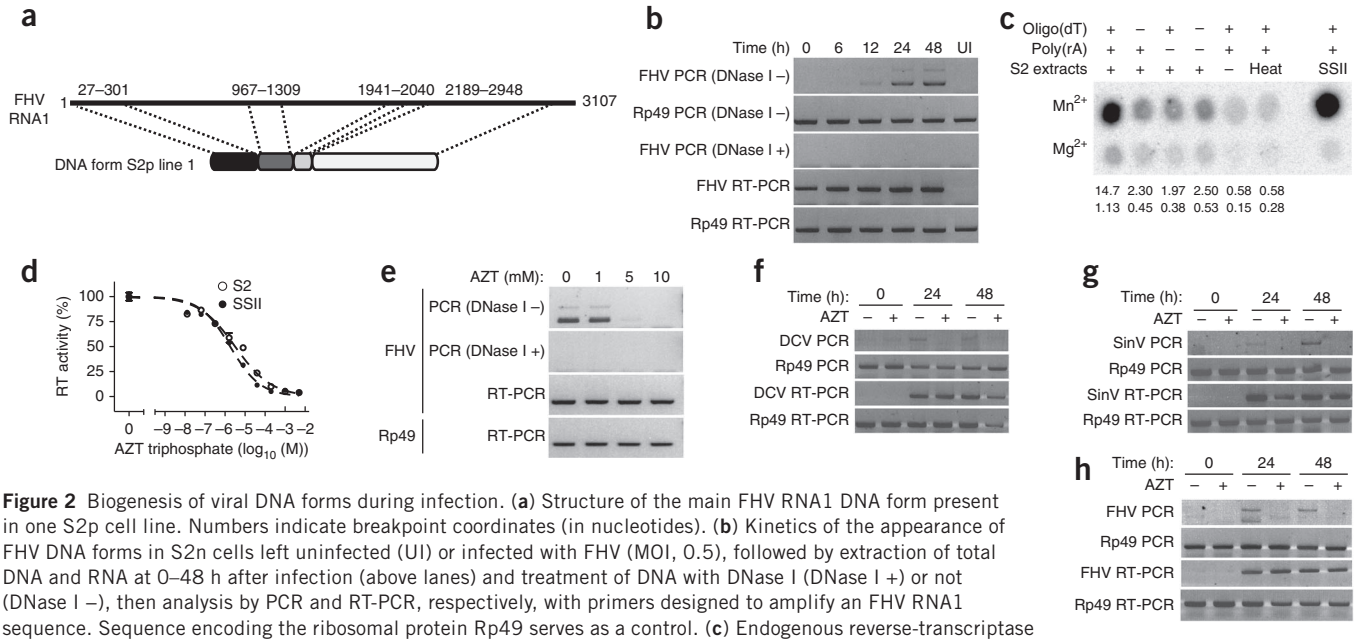

Figure 2 Biogenesis of viral DNA forms during infection. (**a**) Structure of the main FHV RNA1 DNA form present in one S2p cell line. Numbers indicate breakpoint coordinates (in nucleotides). (**b**) Kinetics of the appearance of FHV DNA forms in S2n cells left uninfected (UI) or infected with FHV (MOI, 0.5), followed by extraction of total DNA and RNA at 0–48 h after infection (above lanes) and treatment of DNA with DNase I (DNase I +) or not (DNase I –), then analysis by PCR and RT-PCR, respectively, with primers designed to amplify an FHV RNA1 sequence. Sequence encoding the ribosomal protein Rp49 serves as a control. (**c**) Endogenous reverse-transcriptase activity of S2n cell extracts, Superscript II (SSII, used in place of S2n cell extracts) or heat-inactivated cells (Heat), assessed in the presence of Mg^{2+} or Mn^{2+} (left margin) and various combinations of oligo(dT) and poly(rA) (above), spotted onto DE81 paper (which retains poly(dT) products but not free [^{32}P]dTTP) and measured at initial velocity phase. Below, quantification of the spots above, in arbitrary units. (**d**) Inhibition of the reverse-transcriptase activity of S2n cell extracts or Superscript II by AZT triphosphate *in vitro*. IC_{50} values (half-maximal inhibitory concentration, determined by nonlinear regression): 3.2 μM (S2n endogenous activity) and 1.8 μM (Superscript II). (**e**) Appearance of FHV DNA forms in S2n cells infected with FHV (MOI, 0.5) in the presence (1, 5 or 10 mM) or absence (0 mM) of AZT, then treated as in **b** at 24 h after infection. (**f**–**h**) Kinetics of the appearance of the DNA forms of DCV (**f**), Sindbis virus (**g**) or FHV (**h**) in S2 cells (**f**,**g**) or Kc167 cells (**h**) infected with DCV (**f**), Sindbis virus (**g**) or FHV (**h**) and treated as in **b**. Data are from one experiment representative of eight (**b**), three (**c**,**e**) or two (**f**–**h**) experiments or are from three experiments (**d**; mean and s.e.m.).

from S2 cell lines persistently infected with FHV, DCV or DXV and amplified the DNA with primers complementary to various regions of the viral genomes. All samples contained DNA sequences (**Fig. 2a** and **Supplementary Fig. 2a**,**b**), a result we further confirmed by sequencing. Sindbis virus, an arbovirus that naturally produces persistent infection in insects, also produced a DNA form (**Supplementary Fig. 2c**). When we treated DNA samples with RNase III, a mixture of RNase A and RNAse I, DNase I or exonuclease I, only DNase I precluded the generation of a PCR product (**Supplementary Fig. 2d** and data not shown), which confirmed that the molecular template was a DNA molecule.

Through the use of 'genome walking', we extended the initially identified sequences corresponding to FHV RNA1 and reconstructed the FHV DNA forms present in S2p cell lines (**Fig. 2a** and **Supplementary Fig. 3a**). The DNA form was heavily reorganized, with a major recombinant RNA1 segment considerably shorter than the usual 3,107 nucleotides (**Supplementary Fig. 3a**,**b**). Nonhomologous RNA recombination during negative-strand synthesis of FHV RNA1 and RNA2 could have been the template for those new DNA structures[31]. Alternatively, defective interfering particles could have served as a template[32,33], as the DNA forms had breakpoints and rearrangements similar to those identified in RNA1 defective interfering particles[11]. Of note, we also identified DNA forms derived from FHV RNA2 that were similar in sequence to RNA2 defective interfering particles[11,32] (data not shown). We then infected S2n cells with FHV at a multiplicity of infection (MOI) of 0.5 and monitored the appearance of FHV DNA over time by PCR. DNA forms were detectable as early as 12 h after infection (**Fig. 2b**).

Because reverse transcriptases encoded by retrotransposons and endogenous retroviruses are widespread in insect genomes[34,35], we determined if we could detect reverse-transcriptase activity in S2 cells. We detected robust Mn^{2+}-dependent reverse-transcriptase activity in extracts of S2n cells (**Fig. 2c**). Additionally, we found that such activity was sensitive *in vitro* to the nucleoside reverse-transcriptase inhibitor azidothymidine (AZT) triphosphate to a degree similar to that achieved for a recombinant retroviral reverse transcriptase (**Fig. 2d**). Next we determined whether treating S2n cells with AZT would inhibit the appearance of FHV DNA after infection with FHV. Indeed, AZT triggered a dose-dependent inhibition of FHV DNA in S2n cells infected with FHV at an MOI of 0.5 (**Fig. 2e**). We confirmed that AZT did not impair the growth of S2 cells at the concentrations and time used (**Supplementary Fig. 4a**). Moreover, AZT did not inhibit FHV replication in persistently infected cells in which the DNA form was already present (S2p cells; **Supplementary Fig. 4b**,**c**). Therefore, AZT seemed to be specifically blocking the generation of viral DNA rather than affecting the viability of the cell or virus.

As mitochondrial dysfunction is a known potential side effect of AZT, and as FHV replicates on the mitochondrial external membrane, we also tested the effect of AZT treatment on other viruses, such as DCV and Sindbis virus, whose replication is not associated with mitochondria. In S2 cells, 5 mM AZT also inhibited the synthesis of a viral DNA form after infection with DCV or Sindbis virus at an MOI of 0.5 (**Fig. 2f**,**g**). Finally to rule out the possibility of any effects specific to S2 cells, we also analyzed the generation of FHV DNA forms and its inhibition by treatment with AZT in another *Drosophila* cell line, Kc167. The appearance of FHV DNA after infection of those cells (**Fig. 2h**) indicated that our results were not unique to S2 cells but were instead a general characteristic of insect cells. Thus, during the establishment of viral persistence, RNA viruses and/or their defective interfering particles were reverse-transcribed into viral DNA forms

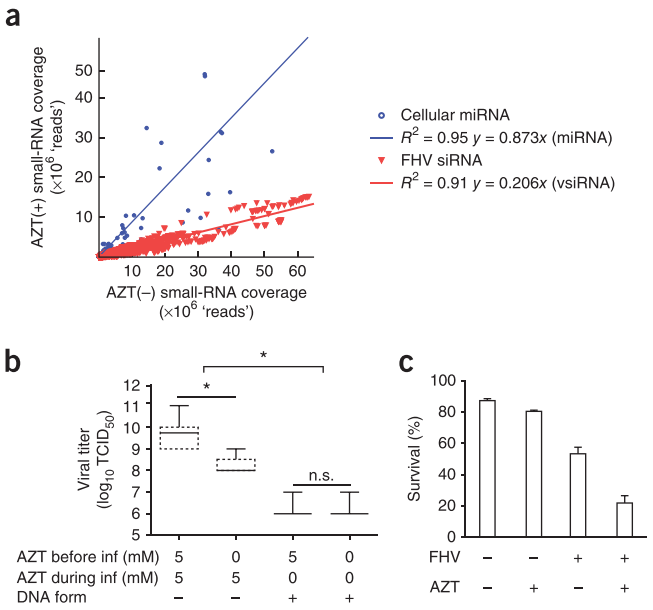

Figure 3 The FHV DNA form improves the antiviral response via the RNAi machinery. (**a**) Accumulation of vsiRNA and cellular miRNA in S2 cells infected for 12 h with FHV in the presence (AZT(+)) or absence (AZT(–)) of AZT, assessed as mapping by small RNA corresponding to each individual miRNA (blue) or to each FHV nucleotide for vsiRNA (red). (**b**) Viral titers in S2 cells given no pretreatment (0) or pretreated (5) with 5 mM AZT (AZT before inf), then infected with serial dilutions of FHV with (5) or without (0) continued AZT treatment (AZT during inf), in the presence (+) or absence (–) of the DNA form (monitored by PCR), determined by end-point dilution (presented as in **Fig. 1f**). (**c**) Survival of S2 cells after infection with FHV in the presence or absence of AZT, measured by exclusion of trypan blue dye. $*P < 0.0001$ (Student's *t*-test). Data are from one experiment representative of two experiments (**a**), at least eight independent experiments (**b**) or three independent experiments with three groups of 500 cells each per condition (**c**; mean and s.d.).

by host reverse transcriptase(s) in cultured *Drosophila* cells of various origins, and AZT inhibited that process.

The viral DNA form mediates persistent infection

To determine whether the absence of a viral DNA form affected the antiviral response during the establishment of persistence, we deep-sequenced small RNAs from FHV-infected S2n cells treated with AZT or not. At similar amounts of viral RNA (**Supplementary Fig. 4d**), the accumulation of vsiRNA was considerably impaired in cells treated with AZT and thus in the absence of FHV DNA forms (**Fig. 3a** and **Supplementary Fig. 4e**). In contrast, the global amount of miRNA remained unchanged despite treatment with AZT (**Fig. 3a**), which indicated that at the doses and time used, AZT did not have pleiotropic effects. We then characterized the sequence diversity of vsiRNA 'reads'. Cells with the DNA form had vsiRNAs that mapped to the junctions of the DNA-form rearrangements, whereas those vsiRNAs were undetectable in cells treated with AZT (**Table 1**). Those results suggested that the FHV DNA form was transcribed and processed into specific vsiRNAs. To determine whether inhibition of the synthesis of FHV DNA and the associated lower amount and diversity of vsiRNAS affected the ability of S2 cells to control FHV replication, we measured viral loads after prolonged exposure to AZT. When the DNA form was inhibited, the viral load was up to 1,000-fold higher than that of infected cells in which the DNA form was present (**Fig. 3b**). That higher viral titer when the appearance of FHV DNA was prevented was accompanied by more cell death (**Fig. 3c**), which indicated that the DNA form was needed to establish persistence. Together these observations emphasized the requirement for the viral DNA form at early time points during infection to improve the antiviral response and to allow the establishment of persistence.

Retrotransposons provide reverse-transcriptase activity

Having linked the appearance of FHV DNA forms to the establishment of persistent infection, we next defined the mechanism by which protection was conferred. We hypothesized that determining the structure and the genomic location of FHV DNA would suggest a mode of action. We thus analyzed the genome of S2p cells by deep sequencing. Analysis of chimeric paired-end 'reads' showed that most viral DNA forms (nine of ten) were fused to fragments corresponding to long-terminal repeat (LTR) retrotransposons, mainly *297*, *blood*, *diver*, *micropia* and *invader2* elements (**Fig. 4a** and **Supplementary Table 1**). That result suggests that FHV RNA was reverse-transcribed by the reverse-transcriptase activity of a broad set of retrotransposons actively transcribed in S2 cells (**Supplementary Fig. 5a**). In some paired-end 'reads', we were able to identify the exact crossover point between *micropia* and FHV DNA (**Fig. 4b** and **Supplementary Fig. 5b,c**). That junction was one nucleotide distant from the end of the LTR of *micropia*, which would suggest a possible 'forced copy-choice' recombination mechanism, as has been proposed for the recombination between retrotransposons and lymphocytic choriomeningitis virus in mice[24]. Because of the repetitive and polymorphic nature of the retrotransposon sequences, we were unable to unambiguously assign chromosomal positions to those FHV DNA forms. Alternatively, the DNA-repair machinery can also process nuclear retroviral DNA to produce stable extrachromosomal circular molecules with a single LTR or two LTRs[36]; thus, we cannot exclude the possibility that the viral DNA form was located on such extrachromosomal molecules. In summary, these results indicated that LTR retrotransposons were the likely source of the reverse-transcriptase activity that produced FHV DNA fragments that were embedded in LTR retrotransposon DNA.

Table 1 Coverage of FHV-FHV junctions by vsiRNA

	FHV siRNA 'reads'	
Junction	AZT (–)	AZT (+)
311–957	5	0
301–967	18	0
318–944	55	0
1263–2275	7	0
1309–1941	10	0
2040–2189	78	0

Abundance of vsiRNA covering FHV-FHV junctions in the presence or absence of AZT. Data are representative of two experiments.

Production of vsiRNAs from newly synthesized viral cDNA

The presence of chimeric DNA molecules consisting of viral cDNA and retrotransposon DNA is not sufficient by itself to explain the mechanism by which persistence is reached. We thus hypothesized that a transcript from the FHV-retrotransposon DNA chimera might produce small RNAs that mediate protection against acute infection through the RNAi machinery, as suggested by the greater number and diversity of vsiRNAs observed (**Fig. 3a,b**). To assess the involvement of RNAi in this process, we depleted S2p cells of Dicer-2 (a core component of RNAi)[18] or CG4572 (an uptake-spread component of RNAi)[37] by knockdown via RNAi and measured cell death. The equilibrium

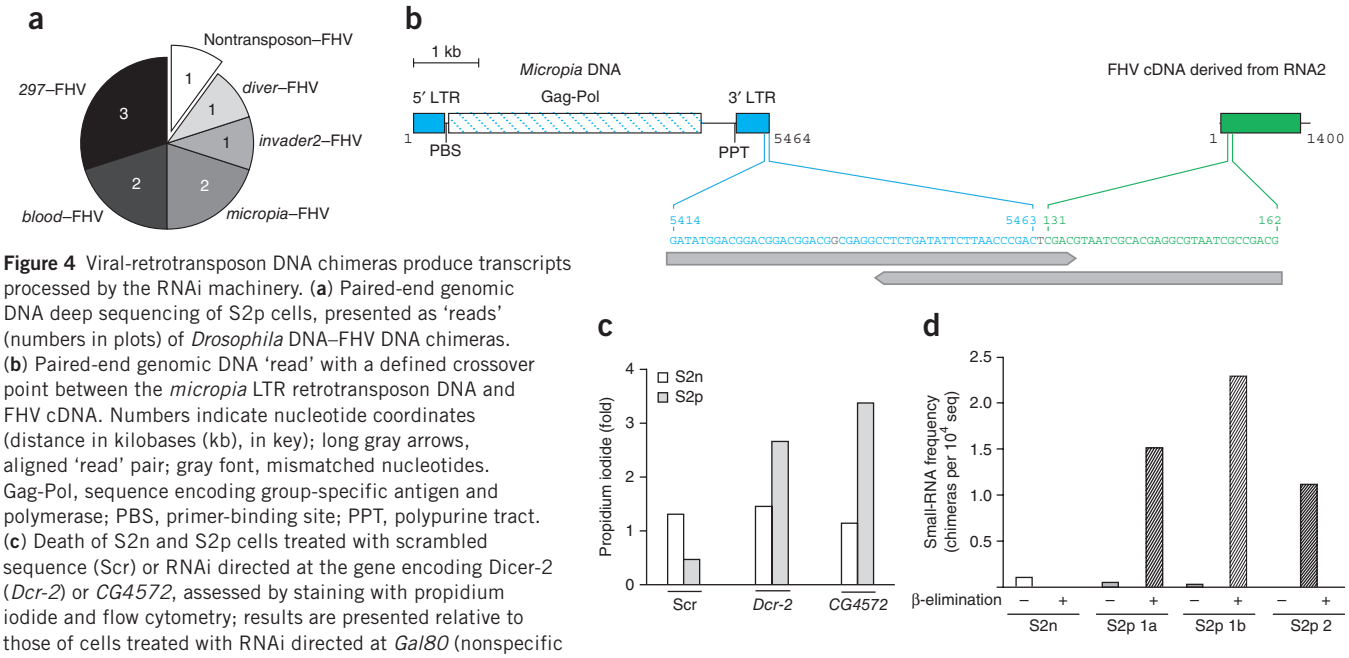

Figure 4 Viral-retrotransposon DNA chimeras produce transcripts processed by the RNAi machinery. (**a**) Paired-end genomic DNA deep sequencing of S2p cells, presented as 'reads' (numbers in plots) of *Drosophila* DNA–FHV DNA chimeras. (**b**) Paired-end genomic DNA 'read' with a defined crossover point between the *micropia* LTR retrotransposon DNA and FHV cDNA. Numbers indicate nucleotide coordinates (distance in kilobases (kb), in key); long gray arrows, aligned 'read' pair; gray font, mismatched nucleotides. Gag-Pol, sequence encoding group-specific antigen and polymerase; PBS, primer-binding site; PPT, polypurine tract. (**c**) Death of S2n and S2p cells treated with scrambled sequence (Scr) or RNAi directed at the gene encoding Dicer-2 (*Dcr-2*) or *CG4572*, assessed by staining with propidium iodide and flow cytometry; results are presented relative to those of cells treated with RNAi directed at *Gal80* (nonspecific control). (**d**) Frequency of small RNA in S2n cells, S2p cells (two independent lines, S2p 1 (technical replicates S2p 1a and S2p 1b) and S2p 2) in the presence (+) or absence (–) of β-elimination, assessed by deep sequencing of RNA libraries for the presence of chimeric sequences mapping partly to the virus and partly to *Drosophila* and presented as chimeras per 1×10^4 total unique sequences (only unique sequences representing at least five 'reads' were included in the analysis). Data are from one experiment (**a**) or three independent experiments (**c**).

between viral replication and persistence was broken in cells in which those genes were silenced by RNAi, which shifted the persistent infection to an acute infection that induced cell death (**Fig. 4c**). To further confirm the involvement of the RNAi response, we generated small-RNA libraries from S2p cell lines. As each vsiRNA could originate from either replicating viral dsRNA (profiles, **Supplementary Fig. 1d–g**) or virus-retrotransposon chimeric transcripts, the only way to discriminate small RNAs specifically from the transcription of the DNA form was to identify those small RNAs whose sequence mapped partly to the virus and partly to the *Drosophila* genome. We expected these chimeric virus-*Drosophila* small RNAs to be very infrequent. To improve detection, we treated the samples to β-elimination (which prevents ligation on the 3′ end of the RNA unless it bears a 3′ modification) to discriminate small RNAs loaded into Ago2 complexes and bearing a 3′ 2′-O-methyl from the total small-RNA background. The frequency at which such virus-*Drosophila* small-RNA chimeras occurred ranged from 1.15 to 2.3 per 10,000 total unique sequences (**Fig. 4d**). Indeed, in S2p cells, we unambiguously identified over 899 chimeric small RNAs that were loaded into Ago2 (241 and 427 for S2p 1 cell lines a and b, respectively, and 231 for the S2p 2 cell line) when we aligned small-RNA libraries with the FHV and *Drosophila* genome reference sequences. We further confirmed the existence of those chimeric small RNAs by analyzing publicly available small-RNA libraries generated from persistently infected S2 cells in other laboratories (**Supplementary Fig. 6**). Of note, in the libraries analyzed, all the chimeric 'reads' mapped to retrotransposons on their *Drosophila* part, and ~65% of their virus-derived sequences matched the positive strand of FHV. Thus, the presence of chimeric

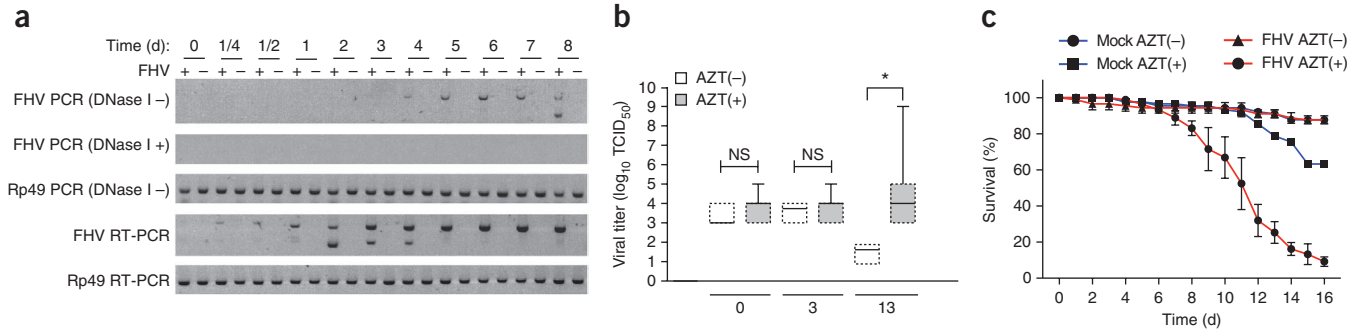

Figure 5 The FHV DNA form is involved in viral persistence *in vivo*. (**a**) Kinetics of the formation of FHV DNA in single wild-type flies injected with Tris-HCl as a control (–) or infected with FHV at a dose of 20 $TCID_{50}$ (+), followed by extraction of DNA and RNA, treatment with DNase I and then PCR and RT-PCR (all as in **Fig. 2b**). (**b**) Viral titers in flies infected with FHV and treated with AZT (AZT(+)) or not (AZT(–)), then homogenized in PBS at 0, 3 and 13 d after infection, determined by end-point dilution (presented as in **Fig. 1f**). $^*P < 0.0001$ (Student's *t*-test). (**c**) Survival of wild-type flies (w^{1118}; $n = 30$ per group) fed 93 mM AZT in sucrose daily (AZT(+)) or not (AZT(–)) and fed Tris-HCl (Mock) or FHV viral stock (FHV) once, monitored daily for 16 d after FHV feeding (horizontal axis). Data are from one experiment representative of four experiments (**a**), at least eight independent experiments with three pools of five flies per pool in each (**b**) or one experiment representative of three experiments with each condition in triplicate (**c**; error bars, s.d.).

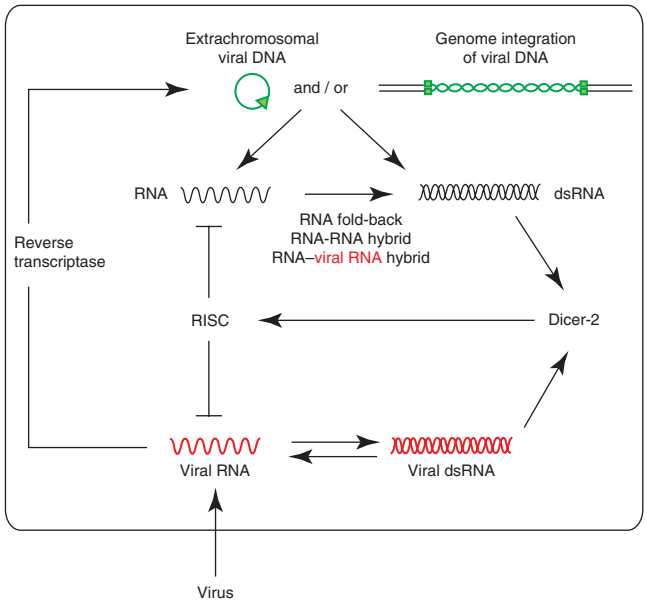

Figure 6 Model for the establishment and maintenance of persistent viral infection in insects. After viral infection, viral genomes (viral RNA) or dsRNA intermediates (viral dsRNA) are propagated (red). Those viral forms are reverse-transcribed by cellular reverse-transcriptase activity into DNA forms (green) that may integrate into the host genome or be processed into extrachromosomal circular DNA. The sequences of viral origin, now in DNA form, will produce transcripts (black) that form dsRNA that is recognized by Dicer-2 and is further processed by a small RNA–related pathway. When viral small RNA from those transcripts reaches the RNA-induced silencing complex (RISC), the ongoing infection is contained and the acute infection is controlled. In this way, both cell and virus progress into a metastable equilibrium that defines the state of persistent infection.

small RNAs that mapped partly to *Drosophila* retrotransposons and partly to FHV further confirmed that the RNA was transcribed from FHV DNA templates and was processed by the siRNA machinery into vsiRNA.

Inhibiting the viral DNA form increases the viral load *in vivo*

To determine if mechanisms similar to those described above could be involved in viral persistence *in vivo*, we infected wild-type flies with 20 $TCID_{50}$ FHV and monitored the appearance of the FHV DNA form over time by PCR of single flies. We detected fragments of FHV DNA *in vivo* from day 4 onward (**Fig. 5a**). Characterization of the FHV RNA1 sequence of those DNA forms identified an almost complete full-length DNA as well as reorganized forms similar to those present in S2p cells (**Supplementary Fig. 3c**). The appearance of a DNA form in infected flies was a common event, with 84.7% of 200 FHV-infected flies having a DNA form and 58% of 200 Sindbis virus–infected flies having a DNA form at day 6 after injection.

To assess the effect of the DNA form on the antiviral response *in vivo*, we developed a protocol for natural inoculation with FHV by feeding. We maintained flies in the presence of 25% sucrose and 93 mM AZT from day 2 after eclosion. At day 4 after eclosion, we fed the flies overnight pure FHV stock (1×10^9 $TCID_{50}$ per ml), then monitored survival every day for 16 d. After that natural infection protocol, we found that flies infected with FHV but not treated with AZT controlled viral infection (**Fig. 5b**) and had a death rate undistinguishable from that of uninfected flies (**Fig. 5c**). In contrast, when treated with AZT, infected flies were unable to contain viral replication, as shown by their high viral titers at day 13 (**Fig. 5b**), and >75% of the flies died within 13 d of infection (**Fig. 5c**). In control experiments, uninfected flies treated with AZT had a low death rate over the course of the experiment, which excluded the possibility of considerable pleiotropic effects of AZT alone (**Fig. 5c**). Of note, we originally developed a double-injection protocol in which we injected flies daily intrathoracically with AZT and challenged them with FHV. This protocol proved to be lethal for the flies beyond 6 d because of repeated physical injury; however, when analyzed, this injection protocol yielded a similar result: in the absence of a DNA form, infected flies died because of an increase in viral replication (data not shown). Collectively, these results confirmed that inhibition of FHV DNA synthesis affected the establishment of persistent infection and demonstrated a role for the DNA form in antiviral immunity *in vivo*. Together our data demonstrated that RNAi and retrotransposons acted together to establish and maintain persistent viral infection in insects; these results provide a mechanistic framework for understanding this process (**Fig. 6**).

DISCUSSION

The host-pathogen interaction triggers selection pressures on both organisms that drive the development of survival strategies. This survival sometimes indicates the incorporation or endogenization of the full parasitic organism by the host, as noted for the endosymbiont bacterium *Wolbachia*, which protects fruit flies and mosquitoes against infection with various viruses[38,39]. In other cases, only part of the parasitic genome is endogenized[26]; for example, bees whose genomes have integrated fragments of Israeli acute paralysis virus are resistant to further challenge with that virus[26]. Our results have demonstrated that one possible root of viral persistence, commonly observed in insects and other arthropods[40], is the endogenization of viral RNA sequences. Indeed, the establishment of persistent viral infection depends on the formation of viral cDNA fragments from which small RNAs are produced by the RNAi machinery. We postulate that viral dsRNA, the canonical substrate of the antiviral RNAi machinery, is also generated from viral cDNA. The biogenesis of that dsRNA remains unknown and should be the subject of future research. However, we speculate that dsRNA might originate from a single-stranded viral transcript generated from the DNA form annealed to the viral genome (either the positive or negative strand, depending on the orientation of the transcript). Another possibility is that a single-stranded viral transcript generated from the DNA form folds back on itself and forms double-stranded secondary structures that could be recognized by Dicer and could enter the RNAi pathway, similar to endogenous siRNA. A third possibility is two complementary single-stranded viral transcripts generated from different loci or by convergent transcription. When the DNA form is inhibited, dsRNA produced through one or several of these mechanisms[3] disappears, with a consequent decrease in vsiRNA.

Given our data, we propose the following model to explain the establishment and maintenance of persistent infection with RNA viruses in insects. After viral infection, ongoing viral replication is limited either by the death of the infected cell or by the antiviral RNAi response in the host. During that process, viral RNA is reverse-transcribed by endogenous reverse-transcriptase activity of LTR retrotransposons. The resulting DNA molecule can then be imported in the nucleus, where retrotransposon-mediated integration into the host genome takes place[34]. Alternatively, the DNA-repair machinery can produce stable extrachromosomal circular DNA molecules that are efficiently transcribed[36]. In all cases, the viral DNA is continuously transcribed and produces dsRNA, which is recognized and processed by the RNAi machinery that boosts the antiviral response.

It is possible that such dsRNA molecules are more exposed to Dicer-2 than are viral replication intermediates, and then the resulting small RNAs are loaded into the RNA-induced silencing complex. When a small RNA that is transcribed and processed from a viral DNA form reaches that complex, the ongoing infection can be better contained and controlled, as the immune response is already primed. In this way, both cell and virus have time to reach a metastable equilibrium (persistent infection).

In the model proposed, the interactions between two parasites (transposon and virus) and the RNAi pathways that control them determine the outcome of the infection. In our model, the basal protection afforded by RNAi during viral infection and the priming of the RNAi response in uninfected cells[37] are key to providing the time the cell needs to initiate the persistence mechanism and to control viral infection. In this way, the virus-transposon interaction serves an important role in the modulation of the immune system: the characteristically massive production of virus followed by cell death in acute infection is compromised, yet viral dissemination in the persistent state is still ensured. We also speculate that in the absence of the canonical production of secondary small RNAs by RNA-dependent RNA polymerase in insects, this mechanism of transformation of viral RNA into DNA, then into RNA and finally into small RNA could be amplifying and maintaining the antiviral immune response throughout the insect's life after primary exposure. By the mechanism proposed, the RNAi immune response is triggered by viral dsRNA replication intermediates and is amplified and boosted through newly generated viral cDNA–derived dsRNA molecules. As defective interfering particles could be the template for new viral DNA synthesis, a similarity to interferon activation in mammalian cells can be seen. Indeed, viruses such as paramyxoviruses can activate the interferon cascade independently of viral protein synthesis but by a mechanism dependent on defective interfering particles[41]. In this model, the integrity of the defective interfering particle genomic RNA seems to be required for efficient interferon induction. In insects, the considerable sequence similarity among FHV DNA forms and defective interfering particles in different S2p cell lines *in vitro*, as well as *in vivo*, suggests a link between defective interfering particles and the biogenesis of viral DNA. Our results are compatible with two possibilities. In one, defective interfering particle RNAs are used as a template by retrotransposon reverse transcriptases to generate viral DNA forms. In the other, viral DNA is the template for the production of defective interfering particles. Further studies addressing this issue could connect defective interfering particles to persistent infections and explain how these are linked.

Until now, endogenization of DNA has been considered a rare event, as it has been assumed that only endogenization in the germline has an effect on host evolution. However, somatic (or 'nontransmissible') endogenization may be much more frequent than expected, as the restrictions on genome integrity in the soma could be more relaxed. DNA forms of nonretroviral viruses have been described in a wide variety of eukaryotic organisms, from plants to mammals[24,25,27–30]. Whether those DNA forms are also involved in immunity mediated by small RNA or other types of immune responses in other organisms is an open question that deserves further exploration. The model proposed here offers a new perspective on antiviral immunity that considers persistent infection the result of the concerted effort of the host's multiple defense pathways.

METHODS

Methods and any associated references are available in the online version of the paper.

Accession codes. NCBI Small Read Archive: SRA045427.

Note: Supplementary information is available in the online version of the paper.

ACKNOWLEDGMENTS

We thank members of the Saleh, Antoniewski and Vignuzzi laboratories for discussions and technical support; M. Vignuzzi, J. Chandler and R. van Rij for critical reading of the manuscript; A. Schneemann (The Scripps Research Institute) for antibody to FHV; P. Vargas for assistance with flow cytometry; and A. Pelisson for advice on retrotransposition. Supported by the French Agence Nationale de la Recherche (ANR-09-JCJC-0045-01 to M.-C.S.), the European Research Council (FP7/2007-2013 ERC 242703 to M.-C.S. and ERC 243312 to G.C.), Institut National de la Santé et de la Recherche Médicale and the Institut National du Cancer (G.C.), the French Ministry of Research (C.M.), La Fondation ARC pour la Recherche sur le Cancer (C.M.) and the AXA Research Fund (J.A.M.).

AUTHOR CONTRIBUTIONS

B.G. and M.-C.S. designed the experiments, discussed the interpretation of the results and wrote the manuscript; G.C. participated in interpreting the data and writing the manuscript; B.G., N.V., J.A.M. and V.G. did research; H.B. generated the genomic DNA and the small-RNA libraries; N.V. and L.F. contributed to the bioinformatics analysis; and C.M., J.V.-O. and G.C. did the *in vitro* analysis of the reverse-transcriptase activity and AZT inhibition.

COMPETING FINANCIAL INTERESTS

The authors declare no competing financial interests.

1. Emerman, M. & Malik, H.S. Paleovirology–modern consequences of ancient viruses. *PLoS Biol.* **8**, e1000301 (2010).
2. Goldstone, D.C. *et al.* Structural and functional analysis of prehistoric lentiviruses uncovers an ancient molecular interface. *Cell Host Microbe* **8**, 248–259 (2010).
3. Goic, B. & Saleh, M.C. Living with the enemy: viral persistent infections from a friendly viewpoint. *Curr. Opin. Microbiol.* **15**, 531–537 (2012).
4. Flegel, T.W. Update on viral accommodation, a model for host-viral interaction in shrimp and other arthropods. *Dev. Comp. Immunol.* **31**, 217–231 (2007).
5. Roekring, S., Flegel, T.W., Malasit, P. & Kittayapong, P. Challenging successive mosquito generations with a densonucleosis virus yields progressive survival improvement but persistent, innocuous infections. *Dev. Comp. Immunol.* **30**, 878–892 (2006).
6. Weaver, S.C. & Reisen, W.K. Present and future arboviral threats. *Antiviral Res.* **85**, 328–345 (2010).
7. Rechavi, O., Minevich, G. & Hobert, O. Transgenerational inheritance of an acquired small RNA-based antiviral response in *C. elegans*. *Cell* **147**, 1248–1256 (2011).
8. Dasgupta, R. *et al.* Replication of flock house virus in three genera of medically important insects. *J. Med. Entomol.* **44**, 102–110 (2007).
9. Dasgupta, R., Selling, B. & Rueckert, R. Flock house virus: a simple model for studying persistent infection in cultured *Drosophila* cells. *Arch. Virol.* (suppl. 9), 121–132 (1994).
10. Li, H., Li, W.X. & Ding, S.W. Induction and suppression of RNA silencing by an animal virus. *Science* **296**, 1319–1321 (2002).
11. Jovel, J. & Schneemann, A. Molecular characterization of *Drosophila* cells persistently infected with Flock House virus. *Virology* **419**, 43–53 (2011).
12. Ebner, P.D., Kim, S.K. & O'Callaghan, D.J. Biological and genotypic properties of defective interfering particles of equine herpesvirus 1 that mediate persistent infection. *Virology* **381**, 98–105 (2008).
13. Tsai, K.N., Tsang, S.F., Huang, C.H. & Chang, R.Y. Defective interfering RNAs of Japanese encephalitis virus found in mosquito cells and correlation with persistent infection. *Virus Res.* **124**, 139–150 (2007).
14. Simon, A.E., Roossinck, M.J. & Havelda, Z. Plant virus satellite and defective interfering RNAs: new paradigms for a new century. *Annu. Rev. Phytopathol.* **42**, 415–437 (2004).
15. Huang, A.S. & Baltimore, D. Defective viral particles and viral disease processes. *Nature* **226**, 325–327 (1970).
16. Marriott, A.C. & Dimmock, N.J. Defective interfering viruses and their potential as antiviral agents. *Rev. Med. Virol.* **20**, 51–62 (2010).
17. Vodovar, N., Goic, B., Blanc, H. & Saleh, M.C. In silico reconstruction of viral genomes from small RNAs improves virus-derived small interfering RNA profiling. *J. Virol.* **85**, 11016–11021 (2011).
18. Flynt, A., Liu, N., Martin, R. & Lai, E.C. Dicing of viral replication intermediates during silencing of latent *Drosophila* viruses. *Proc. Natl. Acad. Sci. USA* **106**, 5270–5275 (2009).
19. Galiana-Arnoux, D., Dostert, C., Schneemann, A., Hoffmann, J.A. & Imler, J.L. Essential function *in vivo* for Dicer-2 in host defense against RNA viruses in *Drosophila*. *Nat. Immunol.* **7**, 590–597 (2006).

20. van Rij, R.P. *et al.* The RNA silencing endonuclease Argonaute 2 mediates specific antiviral immunity in *Drosophila melanogaster*. *Genes Dev.* **20**, 2985–2995 (2006).
21. Wang, X.H. *et al.* RNA interference directs innate immunity against viruses in adult *Drosophila*. *Science* **312**, 452–454 (2006).
22. Belyi, V.A., Levine, A.J. & Skalka, A.M. Unexpected inheritance: multiple integrations of ancient bornavirus and ebolavirus/marburgvirus sequences in vertebrate genomes. *PLoS Pathog.* **6**, e1001030 (2010).
23. Crochu, S. *et al.* Sequences of flavivirus-related RNA viruses persist in DNA form integrated in the genome of *Aedes* spp. mosquitoes. *J. Gen. Virol.* **85**, 1971–1980 (2004).
24. Geuking, M.B. *et al.* Recombination of retrotransposon and exogenous RNA virus results in nonretroviral cDNA integration. *Science* **323**, 393–396 (2009).
25. Klenerman, P., Hengartner, H. & Zinkernagel, R.M. A non-retroviral RNA virus persists in DNA form. *Nature* **390**, 298–301 (1997).
26. Maori, E., Tanne, E. & Sela, I. Reciprocal sequence exchange between non-retro viruses and hosts leading to the appearance of new host phenotypes. *Virology* **362**, 342–349 (2007).
27. Chiba, S. *et al.* Widespread endogenization of genome sequences of non-retroviral RNA viruses into plant genomes. *PLoS Pathog.* **7**, e1002146 (2011).
28. Horie, M. *et al.* Endogenous non-retroviral RNA virus elements in mammalian genomes. *Nature* **463**, 84–87 (2010).
29. Katzourakis, A. & Gifford, R.J. Endogenous viral elements in animal genomes. *PLoS Genet.* **6**, e1001191 (2011).
30. Liu, H. *et al.* Widespread horizontal gene transfer from double-stranded RNA viruses to eukaryotic nuclear genomes. *J. Virol.* **84**, 11876–11887 (2010).
31. Li, Y. & Ball, L.A. Nonhomologous RNA recombination during negative-strand synthesis of flock house virus RNA. *J. Virol.* **67**, 3854–3860 (1993).
32. Zhong, W., Dasgupta, R. & Rueckert, R. Evidence that the packaging signal for nodaviral RNA2 is a bulged stem-loop. *Proc. Natl. Acad. Sci. USA* **89**, 11146–11150 (1992).
33. Wu, Q. *et al.* Virus discovery by deep sequencing and assembly of virus-derived small silencing RNAs. *Proc. Natl. Acad. Sci. USA* **107**, 1606–1611 (2010).
34. Eickbush, T.H. & Jamburuthugoda, V.K. The diversity of retrotransposons and the properties of their reverse transcriptases. *Virus Res.* **134**, 221–234 (2008).
35. Terzian, C., Pelisson, A. & Bucheton, A. Evolution and phylogeny of insect endogenous retroviruses. *BMC Evol. Biol.* **1**, 3 (2001).
36. Wu, Y. & Marsh, J.W. Selective transcription and modulation of resting T cell activity by preintegrated HIV DNA. *Science* **293**, 1503–1506 (2001).
37. Saleh, M.C. *et al.* Antiviral immunity in *Drosophila* requires systemic RNA interference spread. *Nature* **458**, 346–350 (2009).
38. Teixeira, L., Ferreira, A. & Ashburner, M. The bacterial symbiont Wolbachia induces resistance to RNA viral infections in *Drosophila melanogaster*. *PLoS Biol.* **6**, e2 (2008).
39. Bian, G., Xu, Y., Lu, P., Xie, Y. & Xi, Z. The endosymbiotic bacterium Wolbachia induces resistance to dengue virus in Aedes aegypti. *PLoS Pathog.* **6**, e1000833 (2010).
40. Flegel, T.W. Hypothesis for heritable, anti-viral immunity in crustaceans and insects. *Biol. Direct* **4**, 32 (2009).
41. Killip, M.J., Young, D.F., Precious, B.L., Goodbourn, S. & Randall, R.E. Activation of the β interferon promoter by paramyxoviruses in the absence of virus protein synthesis. *J. Gen. Virol.* **93**, 299–307 (2012).

ONLINE METHODS

Cells and cell assays. *Drosophila* S2 cells (Invitrogen) and Kc167 cells were cultured at 25 °C in Schneider's *Drosophila* medium supplemented with 10% heat-inactivated FCS. For cell-proliferation assays, S2 cells were incubated for 15 min at room temperature in the presence of 2 μM CFDA (5- (and 6-) carboxyfluorescein diacetate; Invitrogen) and were washed twice with PBS. For cell-viability assays, 1 μg/ml of propidium iodide was added to the cells, followed by incubation for 5 min at room temperature. Cellular fluorescence of 5×10^4 cells was analyzed at various times after staining with a FACSCalibur and CellQuest software. Alternatively (for **Fig. 3d**), for quantification of the viability of FHV-infected S2 cells in presence or absence of AZT, a portion of the infected cells was removed and stained for 5 min with 0.2% trypan blue (Sigma-Aldrich). For ultraviolet irradiation–induced DNA damage, cells were exposed to increasing doses of ultraviolet irradiation. At 72 h after irradiation, cell viability was measured by CellTiter-Glo Luminescent Cell Viability Assay (Promega).

Viruses. FHV, DCV and DXV viral stocks were prepared on low-passage S2 cells and titers were measured by end-point dilution. S2 cells (25×10^4 cells per well in a 96-well plates) were inoculated with tenfold dilutions of virus stocks. At 7 or 14 d after infection, cytopathic effects were analyzed. Viral titers were calculated as $TCID_{50}$ (half-maximal tissue culture infectious dose) according to a published method[42].

For quantification of viral titers in flies, five flies were homogenized at various time in 250 μL PBS, and titers in the homogenate were calculated as described above.

Sindbis viral stock was prepared in BHK hamster kidney cells and titers were measured by plaque assay.

Fly infection. For infection of flies by injection, w^{1118} flies were used as wild-type controls; these were reared on standard medium at 25 °C. Four-day-old female flies were injected intrathoracically with 50 nl of a FHV dilution in 10 mM Tris-HCl (pH 7.5) as described[43], with a Nanoject II injector. For analysis of survival, FHV was injected at a dose of 500 $TCID_{50}$ per fly. Mock-infected flies were injected with 10 mM Tris-HCl, pH 7.5. Fly mortality at day 1 was attributed to damage produced by the injection procedure and those data were excluded from further analysis. Mortality was monitored daily for 14 d, and every 3–4 d the flies were transferred to fresh food.

For *in vivo* viral DNA detection, 4-day-old female wild-type flies were injected with FHV (20 or 200 $TCID_{50}$ per fly). The appearance of FHV DNA was analyzed by single-fly PCR at 6 and 12 h after infection and daily up to 8 d after infection. To determine the number of flies that generate a viral DNA form after infection with RNA virus, we infected flies with FHV or Sindbis virus or mock infected flies with 10 mM Tris-HCl, pH 7.5. The formation of viral DNA was monitored by single-fly PCR at 6 d after infection with the following pairs of primers: 69F and 1002R for FHV; and NSP1F and 913R for Sindbis virus.

For infection of flies by viral feeding, the following procedure was used for the AZT *in vivo* assay: w^{1118} flies were fed 93 mM AZT in 25% sucrose daily from day 2 after eclosion or were not fed AZT. At day 4 after eclosion, flies were fed a pure stock of FHV (1×10^9 $TCID_{50}$ per ml) or Tris-HCl 10 mM, pH 7.5 (as a control), once overnight. Survival was monitored every day for 16 d. Flies were kept at 25 °C. At various time points, flies were collected and viral titers were calculated as described above.

For single-fly PCR, each fly was homogenized in 50 μl squishing buffer (100 mM Tris-HCl, 25 mM NaCl, 1 mM EDTA, pH 8, and 0.2 mg/ml proteinase K) and incubated for 1 h at 37 °C. Proteinase K was inactivated for 2 min at 95 °C. A portion of the homogenate (1 μl) was treated for 30 min at 37 °C with 10 units of DNase I (Roche) or not, followed by heat inactivation (72 °C for 10 min). A portion of the sample (1 μl, corresponding to 0.1 μl of the original homogenate) was analyzed by PCR.

AZT treatment. S2n or S2p cells (3×10^6) were incubated for 6 h in the presence or absence of 5 mM AZT (Sigma-Aldrich). Cells were then inoculated with a tenfold serial dilution of FHV. At the time of inoculation, AZT was removed or maintained for the rest of the experiment. Viral titers were calculated by endpoint dilution as described above.

S2 cell extracts and assay of reverse-transcriptase activity. S2 cell pellets were washed once with PBS and lysed in CHAPS lysis buffer (10 mM Tris-HCl, pH 7.5, 400 mM NaCl, 1 mM $MgCl_2$, 1 mM EGTA, 0.5% CHAPS and 10% glycerol, supplemented before use with Complete EDTA-free protease inhibitor 'cocktail' (Roche) and 1 mM DTT). After incubation for 10 min at 4 °C, cell debris were removed by centrifugation at 16,000*g* for 10 min at 4 °C. Supernatants were transferred to clean tubes. Total protein concentration was determined by Bradford assay (Biorad). Samples were 'snap-frozen' in liquid nitrogen and were stored at −80 °C until use.

Reverse-transcriptase assays were carried out for 15 min at 25 °C in a reaction volume of 50 μl containing 4 μg S2 cell extracts or 0.05 U Superscript II (Invitrogen), 320 ng oligo(dT) (Invitrogen), 500 ng poly(rA) (GE Healthcare) and 1 μCi [α-^{32}P]dTTP (3,000 Ci/mmol; PerkinElmer) in 50 mM Tris-HCl, pH 7.5, 50 mM KCl, 5 mM $MgCl_2$ or 0.7 mM $MnCl_2$, 5 mM DTT and 0.1% Triton X-100. Then, 5 μl of each reaction was spotted in triplicate onto DE-81 paper (an ion-exchange paper that retains incorporated nucleotides but not free dNTP). Papers were washed five times with 100 ml of 2× saline–sodium citrate solution, followed by exposure to a PhosphorImager screen. The nucleotide analog and reverse-transcriptase inhibitor azidothymidine-triphosphate was from Bioron. Nonlinear regression and determination of half-maximal inhibitory concentration were calculated with Prism 5 software (GraphPad).

Small-RNA and genomic libraries. Small-RNA libraries of S2 cells were constructed as described[44]. For β-elimination, standard procedures were followed[45]. Small RNAs were treated for 10 min at room temperature with 25 mM sodium periodate, followed by β-elimination for 90 min at 45 °C in 50 μL 1× borax buffer (30 mM borax, 30 mM boric acid and 50 mM NaOH, pH 9.5). Only small RNA with 2′-O-methyl at the extremity (a sign of Ago2 loading) that resisted the oxidation treatment were recovered by sequencing. Genomic DNA libraries of S2 cells were generated with Nextera Technology for Next-Generation Sequencing Library Preparation (Epicentre) with a fragment size centered around 400 base pairs. Libraries were sequenced (36 single 'reads' for small RNAs and 2 × 54 paired-end 'reads' for genomic DNA) on an Illumina Genome Analyzer *IIx*. 'Reads' were analyzed with in-house Perl scripts.

Bioinformatics analysis of small-RNA libraries. For the detection of chimeric small RNAs, virus-derived siRNA profiles were generated according a published method[17]. For the identification of chimeric siRNAs, small RNA 'reads' 36 nucleotides in length were clipped for adapters with the FASTX-Toolkit suite (a collection of command line tools), with 'reads' at least 18 nucleotides in length kept and 'reads' in which the adaptor sequence could not be detected discarded. After removal of contaminating sequences (primers, adapters, ribosomal RNA and so on), 'reads' in which the adaptor was clipped (~25×10^6 for S2n and S2p cells, and ~15×10^6 for S2p cells after β-elimination) were grouped by unique sequences (~3.6×10^5 for S2n cells and ~1×10^6 for S2p cells) with an in-house script. Each unique sequence was given a unique identifier followed by the number of sequences that it represented in the library.

First, unique sequences were filtered with Blastall software (National Center for Biotechnology Information) with the parameters '-W 9 -F F -e 1-g F', first against the *D. melanogaster* reference genome (ftp://ftp.flybase.net/releases/FB2010_03/dmel_r5.26) and then against FHV RNA1 and RNA2 (GenBank accession codes NC_004146.1 and NC_004144.1, respectively) and their defective interfering particles (GU393238.1 for RNA1, and GU393239.1, GU393240.1 and GU393241.1 for RNA2). At each filter, all the unique sequences with a high-scoring segment pair above 18 bases with 0 and 1 mismatches were eliminated. This first step eliminates all nonchimeric small RNAs with a good match in either the host genome or the virus genome.

Second, the Blastall software was used with the parameters '-e 100 -W 9 -F F -q -100 -g F' for selection, among the remaining unique sequences, those with 9–12 bases with the most similarity to FHV RNA1 or RNA2 and their defective interfering particles without gaps or mismatches. Unique sequences without similarity or with similarity of more than 12 bases were not selected. A second blast analysis was done on the selected unique sequences with the parameters '-e 10000 -W 9 -F F -q -100 -g F' for selection of the unique sequences with 9–13 bases of similarity with the *Drosophila* reference genome. Unique sequences without similarity or with similarity of more than 13 bases were not selected. Then, an 'in-house' script was used for comparison of the

doi:10.1038/ni.2542

two Blastall series (versus FHV and versus *Drosophila*), with selection of only the unique sequence with at least 1 'hit' against FHV and 1 'hit' against *Drosophila* and whose positions were considered nonoverlapping. Results that allowed 0, 1 and 2 overlapping bases between the two hits were examined for all the unique sequences. Only unique sequences representing at least five 'reads' on the original small-RNA library were retained. This second step was specifically designed to 'fish out' chimeric transcripts with high confidence.

Of note, to detect chimeric small RNAs that unambiguously map partly to *Drosophila* and partly to FHV, we applied very stringent mapping and filtering parameters. By doing this, we may have lost many chimeric 'reads' that were unable to pass the filters, and thus the final numbers are low (**Fig. 4d** and **Supplementary Fig. 6**).

For comparison of small-RNA libraries with or without AZT treatment, the following procedures were used. For miRNA analysis, the mirBase database was used as reference. Mapping was done with Bowtie software, with applying a seed of 21 nts with a maximum of 2 mismatches. Each miRNA was quantified in the presence or absence of AZT with SAMtools. FHV small RNAs were mapped with Bowtie software for the alignment of short DNA sequences, and a maximum of two mismatches was allowed. The mapping of siRNAs was annotated for each position of FHV RNA1.

Silencing assay. S2 cells (~1×10^6) were transfected with dsRNA with Effectene (QIAGEN). The dsRNA was generated by *in vitro* transcription from T7 promoter–flanked PCR products, with. 2 μg dsRNA used per condition in six-well plates with a 2 ml final volume of Schneider's medium. After 3 d of dsRNA treatment, cells stained with propidium iodide, followed by analysis with a FACSCalibur and CellQuest Software.

RNA blot analysis. Total RNA was isolated with TRIzol (Invitrogen). RNA (24 μg) was separated by electrophoresis through 1.5% denaturing agarose gels, then transferred to a Nytran SuperCharge membrane with the Turbo Blotter system (Whatman). RNA was crosslinked to membranes by ultraviolet irradiation (Stratalinker) and was prehybridized for 2 h at 39 °C in ULTRAhyb-oligo buffer (Ambion) . DNA oligonucleotide probes with complementary to FHV RNA1 and RNA3 and to FHV RNA2 were end-labeled with ^{32}P with T4 polynucleotide kinase (Fermentas), then were added to the hybridization buffer, followed by incubation overnight at 39 °C. Membranes were washed several times at 39 °C in 0.1× saline–sodium citrate with 0.1% SDS and then exposed to a PhosphoImager screen. Probes were stripped by boiling of the membrane twice in 0.1% SDS for a second round hybridization with Rp49 as a 'housekeeping' control.

Quantitative real-time RT-PCR. Total RNA was extracted from S2 cells with TRIzol (invitrogen), then 1 μg total RNA was treated with DNase I according to the manufacturer's instructions (Roche). The cDNA was prepared by reverse transcription with iScript Reverse Transcriptase (BioRad) with oligodT and random hexamer primers. Roche Universal Sybr Green Master Mix (Rox) and a StepOne Plus (Applied Biosystems) were used for quantitative RT-PCR. The change-in-threshold values were calculated within the log-linear phase of the amplification curve with the StepOne Plus V2.2.2 software (Applied Biosystems). Quantification was normalized to that of mRNA encoding the endogenous ribosomal protein Rp49. Oligonucleotide primers were as follows:

DNA oligonucleotides (5′ to 3′):
RNA blot:
FHV1 3015-R CTTCCGGTTGTTGGAAGGC
FHV1 2970-R GCGTTCTTCGAGTGTTGGTT
FHV2 701-R CCACCGCTAGAACACCATCT
FHV2 971-R ACCATGCCTTGAGTATGGC
Rp49 465-R ACAAATGTGTATTCCGACCACG
PCR:
FHV1 1-F GTTTTCGAAACAAATAAAACAGAAAAG
FHV1 27-F GCGAACCTACACAATGACTCTA
FHV1 69-F CCAGATCACCCGAACTGAAT
FHV1 1002-R CGACCGATGGAAACCAGCAGTTC
FHV1 1240-R CAGTTGGACTAATTGGTGACAC
FHV1 2537-R AACCTGCTTCATCAAATGGG
FHV1 2674-R CGCCGTCTTCATCAAACGTACA
FHV1 2970-R GCGTTCTTCGAGTGTTGGTT
FHV1 3107-R CCTCTGCCCTTTCGGGCTAGAACGGG
SIN NSP1-F AAGGATCTCCGGACCGTACT
SINV 913-R CCTTCGCAACTCACCACTGT
SIN NSP1-F TCTGCCGATCATAGCACAAG
SIN NSP2-R CTTCTTAACGCAACGCTTC
SIN NSP3-F GGATCAATTTTCGACGGAGA
SIN NSP4-R TTGAATGTCGCTGAGTCCAG
SINV 10299-F AAGGTCTTCGGAGGGGTCTA
SINV 10898-R AATGGGAATGTTCCCGTATG
DCV 724-F CCAGAGGGCGTTGTCGTCTCCCCCT
DCV 1108-R GGGGCGATTGAACGGGTCCAGGG
DCV 3133-F GTTGCCTTATCTGCTCTG
DCV 4328-R CGCATAACCATGCTCTTCTG
DCV 4235-F CGACTCGTACTGGGGATTGT
DCV 4863-R AGGAAATCCTGGTGACGTTG
DXV-A 277-F CGTCGAGTATTAGCGGCTTC
DXV-A 767-R GCCCTACGGAGTCCACATTA
DXV-B 1493-F AGGTTGGACATCGAAACAGG
DXV-B 2175-R GGCTAGCCTCTACGGCTTTT
DXV-B 1812-F TCAAGGCATTCGATCCCTAC
DXV-B 2330-R CCATACGCGTTGTGTATTCG
PCR primers generating dsRNA:
T7 Gal80-F TAATACGACTCACTATAGGGAGAGGGCCCTTGCATGT TCACTAG
T7Gal80-R TAATACGACTCACTATAGGGAGACCTTTGAAACTGCAT GACACTGG
T7 CG4572-F TAATACGACTCACTATAGGGAGACTATAGTCGCAAT AAGCGGAGC
T7 CG4572-R TAATACGACTCACTATAGGGAGATATGGCATTTTGT ACCTTGTGG
T7 Dcr2-F TAATACGACTCACTATAGGGAGAAAGCGGTTGTAGTTG ATATCGC
T7 Dcr2-R TAATACGACTCACTATAGGGAGAAGTACGTATCCCGTA GAGCTGG
Quantitative RT-PCR:
297-F TGGACGGACAAATTACACGA
297-R TCCGATTGGTTACCTTCCAG
blood-F GACCAAAGCCCTTGACCATA
blood-R TACTTCGCACCACGAAGTTG
micropia-F ATATTGTTCGCCCAAGTTGC
micropia-R TAATTTGCTCCGCGAAGTCT
copia-F GGAGGTTGTGCCTCCACTTA
copia-R CTCTTGGAGACGCTTTACGG
mdg1-F AAGCCTGCCTGTTTTCAAGA
mdg1-R TGCTTCACTCTGACCCTCCT
gapdh-F TGATGAAATTAAGGCCAAGGTTCAGGA
gapdh-R TCGTTGTCGTACCAAGAGATCAGCTTC
rp49-F ATCGGTTACGGATCGAACA
rp49-R ACAATCTCCTTGCGCTTCTT
FHV1-F CCAGATCACCCGAACTGAAT
FHV1-R AGGCTGTCAAGCGGATAGAA

42. Reed, L.J. & Muench, H. A simple method of estimating fifty per cent endpoints. *Am. J. Hyg.* **27**, 493–497 (1938).
43. Cherry, S. & Perrimon, N. Entry is a rate-limiting step for viral infection in a *Drosophila melanogaster* model of pathogenesis. *Nat. Immunol.* **5**, 81–87 (2004).
44. Gausson, V. & Saleh, M.C. Viral small RNA cloning and sequencing. *Methods Mol. Biol.* **721**, 107–122 (2011).
45. Vagin, V.V. *et al.* A distinct small RNA pathway silences selfish genetic elements in the germline. *Science* **313**, 320–324 (2006).